Physical Reservoir Computing Using Nonlinear MEMS Resonator Having High Memory Capacity at "Edge of Chaos"

AUTHOR(S):

Takemura, Hiroki; Mizumoto, Takahiro; Banerjee, Amit; Hirotani, Jun; Tsuchiya, Toshiyuki

CITATION:

Takemura, Hiroki ...[et al]. Physical Reservoir Computing Using Nonlinear MEMS Resonator Having High Memory Capacity at "Edge of Chaos". 2023 IEEE 36th International Conference on Micro Electro Mechanical Systems (MEMS) 2023: 515-518

ISSUE DATE:

2023

URL:

http://hdl.handle.net/2433/284807

PHYSICAL RESERVOIR COMPUTING USING NONLINEAR MEMS RESONATOR HAVING HIGH MEMORY CAPACITY AT "EDGE OF CHAOS"

Hiroki Takemura, Takahiro Mizumoto, Amit Banerjee, Jun Hirotani, and Toshiyuki Tsuchiya
Department of Micro Engineering, Kyoto University, JAPAN

ABSTRACT

This paper reports physical reservoir computing (PRC) using a single nonlinear electrostatic resonator and demonstrates its high memory capacity at "edge of chaos." The resonator is a simple doubly supported resonator fabricated from a silicon-on-insulator wafer. We proposed a PRC system without feedback loop, in which its memory capacity relies on the decay time of the high-Q resonator. The benchmark task results indicate that the system shows good linear and nonlinear memory capacities at the resonance and the maximum capacity was obtained at the vicinity of the instability edge of the frequency response.

KEYWORDS

Physical reservoir computing, electrostatic, nonlinear resonator, machine learning, silicon-on-insulator.

INTRODUCTION

Physical reservoir computing (PRC) is one of the machine learning algorisms where the inner layer of recurrent neural network (RNN) is implemented by nonlinear physical system. Figure 1 shows a human motion recognition system as an example. Vibration signal detected by accelerometer input to a recurrent neural network and outputs classifies person's activity, such as sitting, standing, walking, and running. Training of a conventional RNN is time- and power-consuming because of its complicated network structure and difficulties in optimizing all the node transfer functions and the connection weights, which makes difficult to implement it to portable systems. In the reservoir computing, the hidden (middle) layer of RNN is fixed (called as a reservoir) and only the weights of output layer are optimized by such as linear and Ridge regression methods. PRC employs a nonlinear physical system for the reservoir, such as optical, spintronic, thermal, and electrical systems. A microelectro-mechanical nonlinear resonator is one of the candidates for the reservoir and experimental demonstration results have been reported [1-4]. One of the features of MEMS reservoir is that its integration to MEMS sensors [4] and mechanical signal processing is conducted before transduction to electrical signal, which greatly reduces the power consumption of remote sensing systems. We have utilized a frequency modulated capacitive accelerometer to a sensor-integrated physical reservoir. The doubly clamped beam resonator for acceleration detection was used as a physical reservoir with its enhanced nonlinearity and the delayed feedback loop. The vibration inputs were successfully processed by machine learning tasks and the results showed good performances [4]. However, the design strategy and parameter optimization procedure of MEMS resonator for PRC have not been investigated and clarified owing to its complicated output.

In this study, we use a simple nonlinear resonator driven by electrostatic force and detected by capacitance change and do not use the delayed feedback loop, which is often used in MEMS reservoir [1,4]. The memory capacity is obtained by controlling its Q-factor and time constant operated in a vacuum environment. Benchmark tasks were conducted by changing the oscillation frequency and sampling time to study its optimal memory capacities.

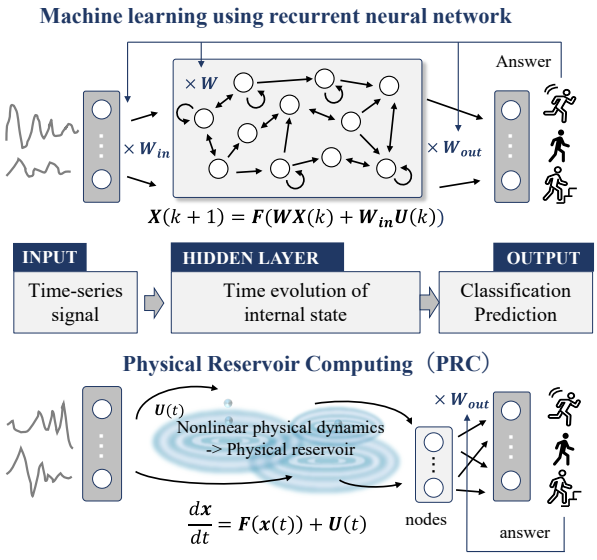

Figure 1: Concept of physical reservoir computing.

MEMS RESERVOIR

Figure 2 shows the nonlinear electrostatic resonator used as a reservoir in this study. The resonator has a pair of doubly clamped beams of 330 μm long and 3 μm wide, which shows the hard spring effect because of the axial force on the beams. There are two pairs of parallel plate

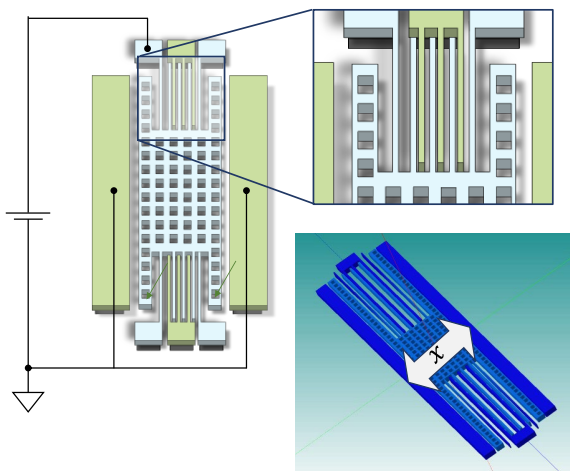

Figure 2: Electrostatic nonlinear SOI resonator as a physical reservoir.

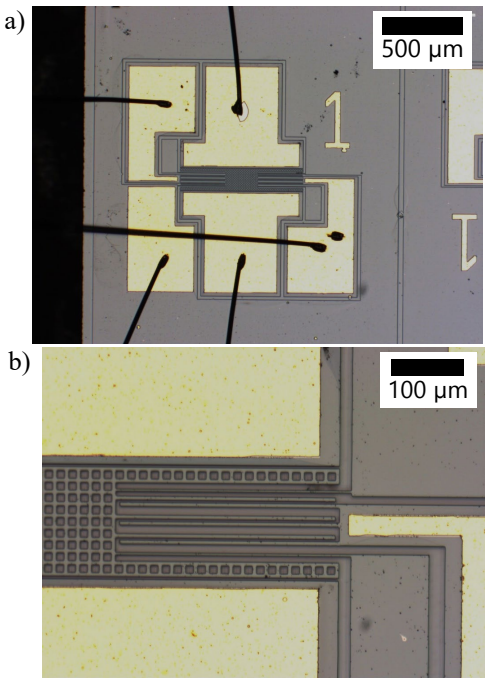

Figure 3: Fabricated SOI nonlinear resonator. a) Optical microscope image of resonator. b) Close-up view of doubly supported beams and parallel plate displacement sensor.

capacitances. The one pair on the left and right sides of the mass whose length is 700 μm is for actuation. The other pair on the top and bottom is for displacement detection. There are three capacitances on each side and the length is 275 μm. The gaps of these electrodes are 3 μm. The thickness is 15 μm. The resonant frequency at the first mode was designed and simulated as 11.96 kHz.

The resonators were fabricated on 4-inch silicon-on-insulator (SOI) wafer with 15-μm-thick device and 2-μm-thick buried oxide layers. A standard fabrication process using contact lithography and Bosch process (Samco, RIE-800iPB) for patterning the device layer and vapor HF etching (SPTS, MLT-SLE-Ox) for sacrificial etching. An Au/Cr layer is used for electrodes. A fabricated reservoir resonator is shown in Fig. 3.

RC ARCHITECHTURE

The reservoir computing architecture is shown in Fig. 4. The input is added as a bias voltage to the oscillation ac signal at a frequency near the resonant frequency. The oscillated vibration is detected at the displacement-detecting capacitance as a current by a biasing voltage applied on the mass. The reservoir output is just taken from the envelope of the vibration velocity signal as an output of transimpedance amplifiers (TIAs). The state variable vector $\boldsymbol{X}_{\mathrm{k}}$ is acquired from the envelope waveform of the enveloped signal at a constant interval T. The vector dimensions were set to 100, which means that the hundred envelope values as virtual nodes were extracted at a constant interval at $T/100$, which are indicated as yellow points on the enlarged velocity plot in Fig. 4.

In the benchmark tasks, m random binary input data was input to the reservoir and the state matrix $\boldsymbol{X}$ was collected. The output data $\boldsymbol{Y}$ is calculated by multiplying the weight matrix $\boldsymbol{W}$ of a 100th order vector. In the teaching step, a certain number of inputs are processed in the RC. The weight values are determined by the Ridge regression;

$$\boldsymbol{W} = \bar{\boldsymbol{Y}}\boldsymbol{X}^T(\boldsymbol{X}\boldsymbol{X}^T + \lambda\boldsymbol{I})^{-1} \quad (1)$$

$\bar{\boldsymbol{Y}}$ is the answer for the inputs and λ is a constant. In the testing step, The outputs $\boldsymbol{Y} = \boldsymbol{X}\boldsymbol{W}$ were collected and compared with the answer $\bar{\boldsymbol{Y}}$.

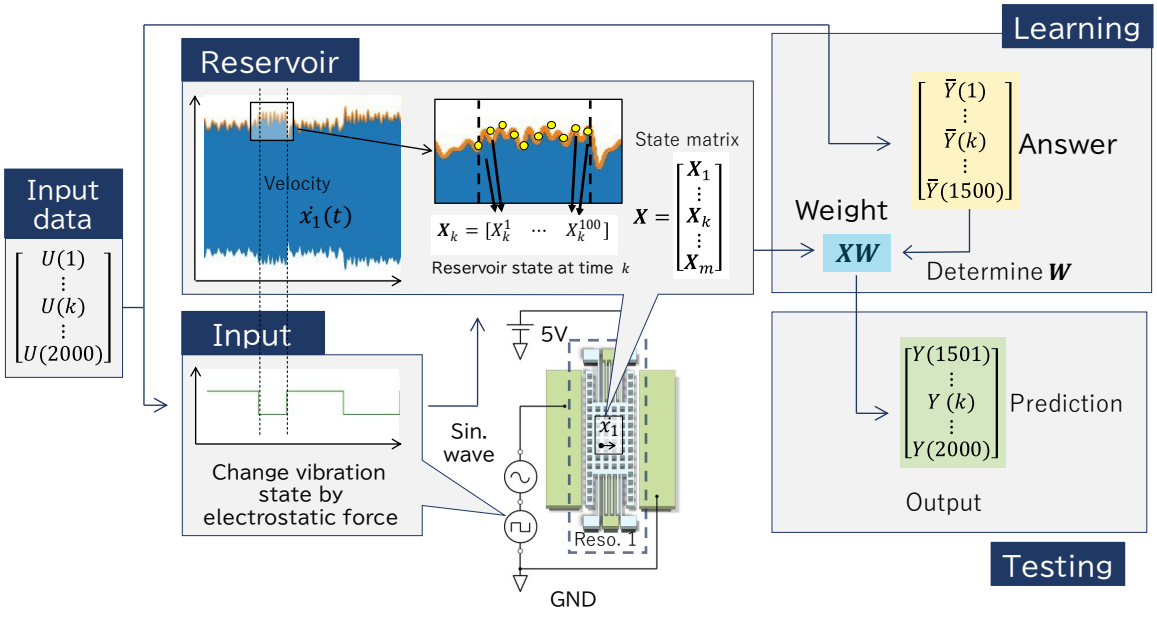

Figure 4: Schematic diagram of reservoir computing architecture for benchmark tasks.

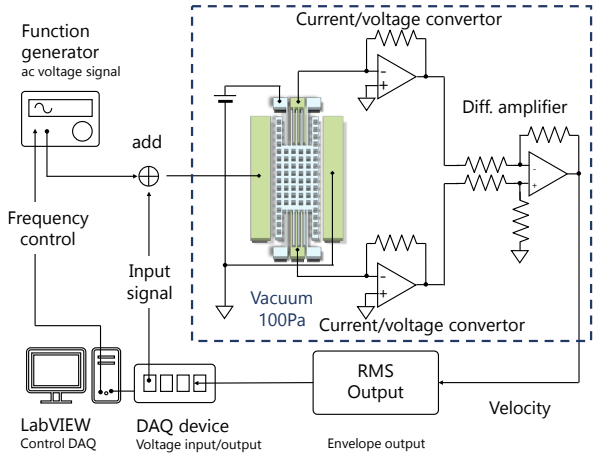

Figure 5: Experimental setups for RC.

EXPERIMENTAL

Data collection

Figure 5 shows the experimental setup for reservoir computing. The ac oscillation signal was generated using function generator controlled by LabVIEW and input signal was added by an op-amp and applied to the reservoir resonator for electrostatic oscillation. The displacement velocity was detected by the TIAs and differential amplifier. The rms-dc convertor (AD736, Analog Devices) was used to convert the velocity signal to the envelope with the time constant of 1 ms. The rms output of 2000 inputs was acquired and then the acquired data was processed offline.

Benchmark tasks

Benchmark tasks to evaluate memory capacity were conducted, as shown in the diagram in Fig. 4. We employ the parity check task (nonlinear memory) and the short memory task (linear memory). Main purpose of the benchmark tasks is to confirm machine learning capability. We defined the memory capacity MC;

$$MC = \sum_{n=0}^{\infty} [\mathrm{Corr}(\bar{\boldsymbol{Y}}_{\boldsymbol{n}}, \boldsymbol{Y}_{\boldsymbol{n}})]^2 \qquad (2)$$

where n is the order of the benchmark tasks, $\boldsymbol{Y}_{\boldsymbol{n}}$ is the estimated answer of n-th-order task, and Corr( ) means the correlation coefficient. In this study, m = 2000 data is processed and the first 1500 data was used for teaching and the later 500 data was used for testing.

The tasks were conducted with the oscillation frequency and the input duration time T as parameters. The ac oscillation amplitude was 1 Vpp and the binary inputs were applied as ±1 V. The mass is biased at 5 V. The oscillation frequency was changed from 90% to 120% of the defined center frequency near the resonant frequency. The ambient pressure on the benchmark task was 100 Pa, so that the response time constant becomes 10 ms. The input holding time is from 2 to 30 ms with 2 ms interval.

RESULTS AND DISCUSSION

Nonlinear frequency response

Figure 6 shows the frequency responses at different oscillation amplitudes at 5 Pa. The resonant frequency was 9.74 kHz and the Q-factor was 3000 at small amplitude but the resonant frequency increased up to 12 kHz by the hard spring effect. The resonant frequency was lower than the design. The reason was fabrication error. The measured beam width was 2.6 μm.

Benchmark task

Figures 7 show the heat map of the correlation coefficient MC of each task as functions of normalized operating frequency Ω and the input holding time T. The square points in Fig. 7a show the rms output at the end of the benchmark task at the input duration of 4 ms. The frequency responses of upward and downward sweep are drawn with the continuous and broken curves. The plot indicates that the vibration kept at the upward sweep state during the task.

The memory capacity map of STM task shows a radial pattern centered at Ω =0.98 and higher capacities are observed at $\Omega = 1.19$, just before the amplitude drops (Fig. 7b). The similar features are seen in that of PC task, but in the radial pattern, the point of high capacity in STM have low capacity in PC, and *vice versa*. These features indicate two rules of thumb about the performance of PRC. First, the memory capacities are complemental between the STM and PC tasks, at the parameters where the linear capacity is high, the nonlinear one is low. Second, the maximum capacities in both tasks were obtained near the unstable point in the frequency response at $\Omega = 1.19$, which is called as "edge of chaos." This is a well-known empirical feature of PRC that the performance become better near the boundary of chaotic responses.

To examine the reason of high capacity at the "edge of chaos" the transient responses at the holding time of 18 ms at the frequency was plotted in Fig. 8. Compared to the

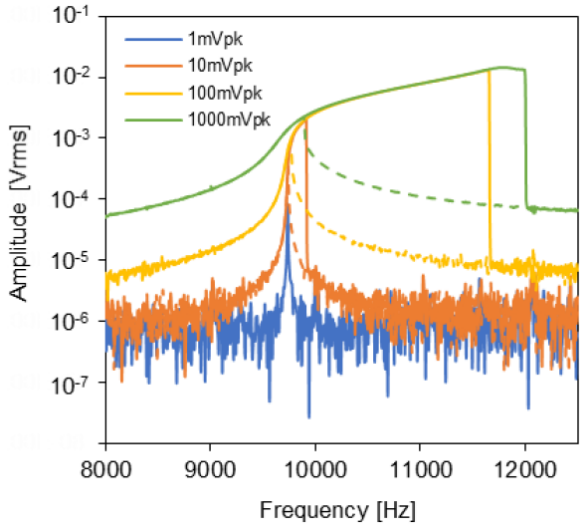

Figure 6: Measured frequency responses of reservoir resonator at different oscillation voltages. Measured at 5 Pa.

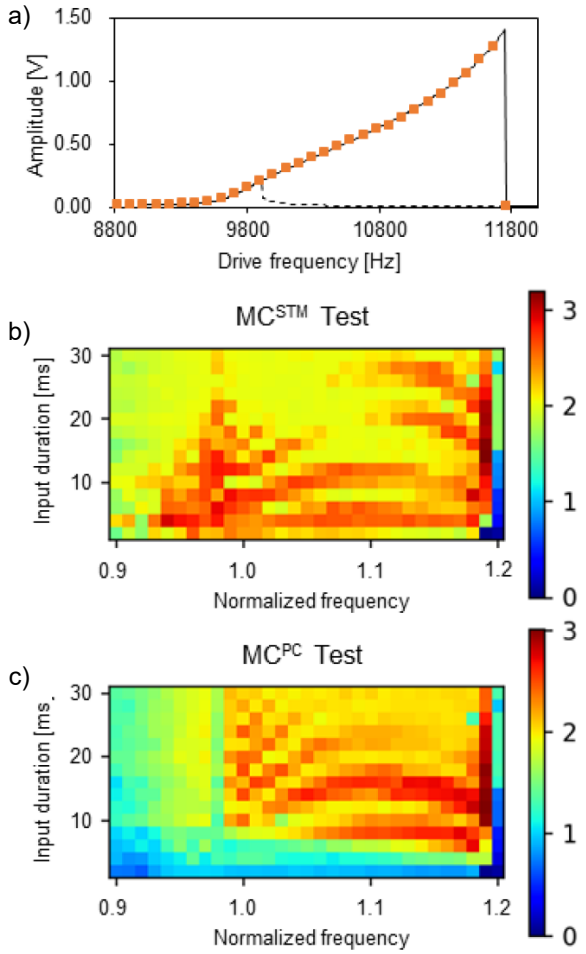

Figure 7: Benchmark results of linear and nonlinear task. a) Frequency response of reservoir resonator, b) heatmap of memory capacity in short term memory task and c) memory capacity in parity check task.

lower operating frequency, Ω=1.19 shows distorted and fluctuated waveforms, which means that the system has the proper complexity in the output signal.

CONCLUSION

We demonstrated that the simple nonlinear MEMS capacitive resonators can be applicable for PRC. The machine learning tasks were successfully conducted experimentally. The memory capacity of the device shows the "edge of chaos" empirical rules. To increase the performance, we are going to evaluate a nonlinear resonator array as a physical reservoir.

ACKNOWLEDGEMENTS

This work is supported by JSPS KAKENHI Grant Numbers JP22K18289, Tateisi Science and Technology Foundation, The Telecommunications Advancement Foundation, and Kyoto University Nanotechnology Hub in the "ARIM Project" sponsored by MEXT, Japan.

REFERENCES

[1] G. Dion, S. Mejaouri, and J. Sylvestrea, Reservoir computing with a single delay-coupled non-linear mechanical oscillator, *Journal of Applied Physics*, 124 (2018), 152132.

[2] M. H. Hasan, A. Al-Ramini, E. Abdel-Rahman, R. Jafari, and F. Alsaleem, Colocalized Sensing and Intelligent Computing in Micro-Sensors, *Sensors*, 20 (2020), 6346

[3] J. Sun, W. Yang, T. Zheng, X. Xiong, Y. Liu, Z. Wang, Z. Li, and X. Zou, Novel nondelay-based reservoir computing with a single micromechanical nonlinear resonator for high-efficiency information processing, *Microsyst. Nanoeng.*, 7 (2021), 83.

[4] T. Mizumoto, Y. Hirai, A. Banerjee, and T. Tsuchiya, MEMS Reservoir Computing using Frequency Modulated Accelerometer, *IEEE MEMS2022*, Tokyo (2022) pp. 487-490.

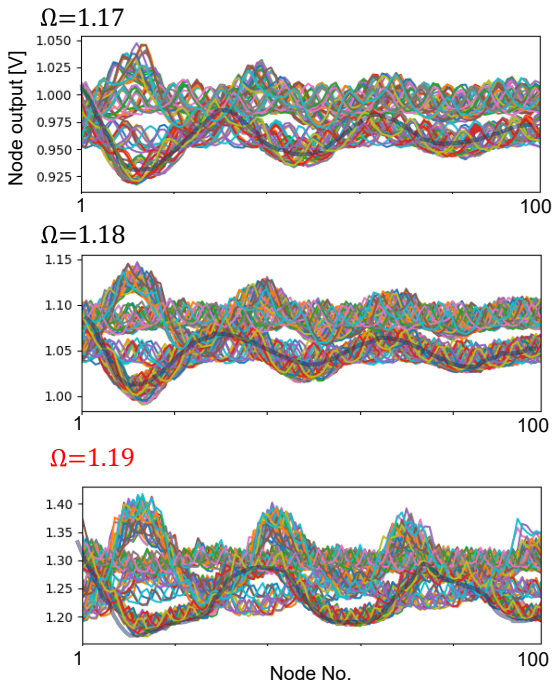

Figure 8: Envelopes of transient responses $\boldsymbol{X}_k$ at the oscillation frequencies Ω of 1.17, 1.18, and 1.19.

CONTACT

*T. Tsuchiya, tel: +81-75-383-3690;
tutti@me.kyoto-u.ac.jp